



A NEW FIBER OPTIC POLARIZER

Moustafa H. Aly

Department of Engineering Mathematics and Physics
Faculty of Engineering
University of Alexandria
Member of the Optical Society of America (OSA)

Abstract-The polarization selective evanescent field coupling of an optical wave in tapered fibers to surface plasmon polaritons supported by a thin aluminium film is experimentally investigated. The results obtained led to the realization of a readily manufacturable, high extinction ratio fiber optic polarizer.

1. INTRODUCTION

Polarization management is required to avoid signal fading and error in coherent fiberoptic communications (e.g. for polarization diversity)and in numerous interferometric sensors such as the fiber optic gyroscope. Polarizing components are essential to such systems. The use of bulk optic polarizing arrangements or integrated optics techniques suffers from high cost, high loss (particularly in the former), and mechanical instability.

In-line all fiber components are more desirable. Several developments, involving polarization selective coupling to structures arranged to interact with the evanescent field of the fibers, have been reported [1-4]. In particular, the polarization selective evanescent field coupling from a fiber to surface plasmon polarization supported by a metal-dielectric interface has featured strongly in such developments [2-4].

In the present work, the model investigated is a thin metal sandwiched between two dielectrics, Fig. 1-a. To achieve the coupling of the surface plasmons, it is necessary to expose the evanescent field around the circumference of the fiber and then to coat a large portion of this area with the required metal film. For this purpose, in our work, the evanescent field has been exposed by tapering the fiber, Fig. 1-b. This is the first time to use a tapered fiber to design a fiber optic polarizer. Four fibers, with different taper lengths L and different waist diameters D , were investigated after appropriate metal coatings have been applied.

2. THE NATURE OF SURFACE PLASMON POLARITONS

Surface plasmon polaritons are wave-like phenomena comprising electromagnetic fields (at optical frequencies) coupled to electron density oscillations at a metal-dielectric interface. The waves are guided by the interface. Writing the wave equation for each side of the interface, imposing the waveguiding boundary conditions, and solving yield a guided (or bound) transverse magnetic TM mode and a radiative TM mode. The later solution exhibits exponentially growing fields into both the metal and the dielectric with no localized field peak. This field distribution is indicative of a radiative mode which cannot be excited by a real source. The electric field distribution (mode profile) associated with the former solution peaks on

FEB. 20 - 22, 1990

the interface and decays exponentially into both the metal and the dielectric material. This is consistent with a bound mode guided by the interface. A metal-dielectric interface is thus a planar waveguide which can support coupled electromagnetic-electron density waves known as surface plasmon polaritons. A thin metal film, the thickness of which is less than the skin depth at the wavelength of interest, can be regarded as a pair of coupled plasmon waveguides.

3. THEORY

Previous analyses [5-6] of the planar waveguiding properties of a thin metal film (index n_2) sandwiched between two dielectrics of indices n_1 and n_3 had provided the following dispersion equation for the effective index n_e of a mode in the structure:

$$k_0 t (n_e^2 - n_2^2)^{\frac{1}{2}} = \tanh^{-1}(A_1) + \tanh^{-1}(A_3) \quad (1)$$

where t is the metal film thickness, $k_0 = 2\pi/\lambda$, λ is the wavelength, $n_e = \beta/k_0$ (β being the propagation constant of the mode) and A_1 and A_3 are given by:

$$A_1 = -(n_2^2/n_1^2)(n_e^2 - n_1^2)^{\frac{1}{2}}/(n_e^2 - n_2^2)^{\frac{1}{2}} \quad (2)$$

It was shown that [7], for efficient coupling, the lower limit of thickness is approximately 100 \AA , and for a polarizer operation the high extinction ratios should be observed for metal thickness $t > 100 \text{ \AA}$ in combination with overlay index $n_3 < 1.451$.

4. APPARATUS

The equipment used for the main set of results is as shown in Fig. 2. The deposition process for the thin metal film was carried out for all tapers with aluminum to a thickness of 200 \AA . This thickness achieves a polarization operation as mentioned before. The laser diode operates at $1.3 \mu\text{m}$, the d.c. bias was set at 105 mV and a square wave a.c. bias of 12 mV was then applied for the ease of measuring output. The polarization controller consists of two independently rotatable fiber loops. This works by creating small amounts of birefringence in the fiber. With the input and output fibers rigidly clamped, a completely universal polarization controller can be realized [8]. The detector is Germanium based and its output is fed into a lock-in amplifier.

Before aligning the system, the plastic coating is stripped from the ends of the fiber and the fiber ends are cleaved to give end faces which are perpendicular to the axes of the fiber. The fiber is aligned to the pigtail from the laser diode using an x-y-z stand. The fiber output can be easily lined up to the relatively large area of the photodiode which is approximately 1 mm^2 .

5. EXPERIMENTAL PROCEDURE

Using the set-up shown in Fig. 2 , the characteristics of the fibers for various capping indices are to be investigated . Capping index oils in a step of 0.002 with an accuracy of ± 0.0005 were used . Upon applying each capping, the polarization controller is used to obtain a maximum and a minimum signal for each refractive index . The reading of the lock-in amplifier , in mV , is proportional to the signal power . After each oil has been applied , it is removed by washing the fiber with Propanol and then removing the excess using compressed air .

For the experimental data we wish to calculate the absorbed power ratios **AE** and **AM** for both **TE** and **TM** modes . The power ratios are defined as :

$$AE = 1 - \frac{\text{Maximum signal power for a specific index}}{\text{Maximum signal power for no capping layer}} \quad (3)$$

$$AM = 1 - \frac{\text{Minimum signal power for a specific index}}{\text{Maximum signal power for no capping layer}} \quad (4)$$

Then the ratio of the maximum to the minimum , for a specific index , is taken as the extinction ratio .

6. RESULTS AND DISCUSSION

The optical fibers used in this work are of 10 and 125 μm core and clad diameters , respectively . The tapered regions are of waist diameters 39.61, 30.06 , 27.17 and 25.42 μm with corresponding lengths 10 , 11 , 12 and 13 mm, respectively . All these dimensions were accurately measured using a giant microscope .

The set-up shown in Fig. 2 was adjusted to give a maximum reading of 500 mV in the lock-in amplifier for no capping layer . Then for each capping oil the maximum and minimum readings were recorded and for both the absorbed power ratio was calculated using Eq. 3 and Eq. 4 . The results are displayed in Fig. 3 for **TE** mode and in Fig. 4 for **TM** mode . From the two figures we can see that the absorption ratio increases with the increase of the taper length. This is physically accepted because when the taper length increases , the waist diameter decreases leading to a high evanescent field and hence high absorbed power .

The polarization sensitivity can be well studied from Fig. 5 which displays the extinction ratio , on a log scale , against the overlay refractive index n_o . From Fig. 5 , we can see that the polarization sensitivity is negligible for tapers of 10 and 11 mm length , then starts to appear in the taper of length 12 mm , but in the taper of length 13 mm the polarization sensitivity is very clear , high extinction ratio . This was expected because the absorbed power increases with the increase of taper length as mentioned .

We can also see a polarization region existing in the range 1.444-1.465 , with a peak at $n_3 = 1.446$ for the 12 mm taper and another at $n_3 = 1.450$ for the 13 mm taper .

The values obtained , especially in case of the 13 mm taper , for the peak of the extinction ratio (≈ 50) are in good agreement with that theoretically predicted for aluminium thickness $> 100 \text{ \AA}$ (7) .

7. CONCLUSION

With the aid of the previous results , it is easily seen that the polarization sensitivity increases with the increase of the taper length L . It also depends on the refractive index of the capping oil n_3 with a peak at $n_3 = 1.450$.

For the best design of a fiber optic polarizer , with aluminium thickness 200 \AA , the taper length must be 13 mm and the overlay refractive index must be 1.450 .

The values obtained for L and n_3 make it easy to design an inexpensive fiber optic polarizer which can be used in :

- i) fiber optic interferometric sensors ,
- ii) coherent telecommunications for polarization diversity receivers , and
- iii) fiber optic gyroscopes .

8. ACKNOWLEDGMENTS

Prof. B.Culshaw , Dr. W.Johnstone and Dr. G.Thursby , University of Strathclyde , Glasgow ,UK , are acknowledged . They kindly helped me,during my research in their university laboratories , to carry out this work .

9. REFERENCES

- [1] R.A.Bergh , H.C.Lefevre and H.J.Show , " Single mode fiber optic polarizer " , Optics Letters , vol. 11 , p. 479 , 1980 .
- [2] T.Hosaka , K.Okamoto and J.Edahiro , " Fabrication of single mode fiber type polarizer " , Optics Letters , vol. 8 , p. 124 , 1983 .
- [3] O.Parriaux , S.Gidon and F.Cochet , " Fiber optic polarizer using plasmon-guided wave resonance " , Conf.Proc. 7th ECOC , p. 6 , 1981 .
- [4] D.Gruchmann , K.Petermann , L.Staudigel and E.Weidel , " Fiber optic polarizers with high extinction ratio" , E.Conf.Proc.9th ECOC,p.305,1983.
- [5]G.Stewart,W.Johnstone,B.Culshaw and T.Hart,Conf.Proc.OFS 88,ThEE2, 1988.
- [6] J.J.Burke and T.Tamir , Phys.Rev.B,vol.33,p. 5186 , 1986 .
- [7] W.Johnstone,G.Stewart,B.Culshaw and T.Hart,"Fiber optic polarizers and polarizing couplers " , Electronics Letters ,vol.24,No.14,p.866,1988.
- [8] H.C.Leferve , Electronics Letters , vol. 16 , p. 778 , 1980 .

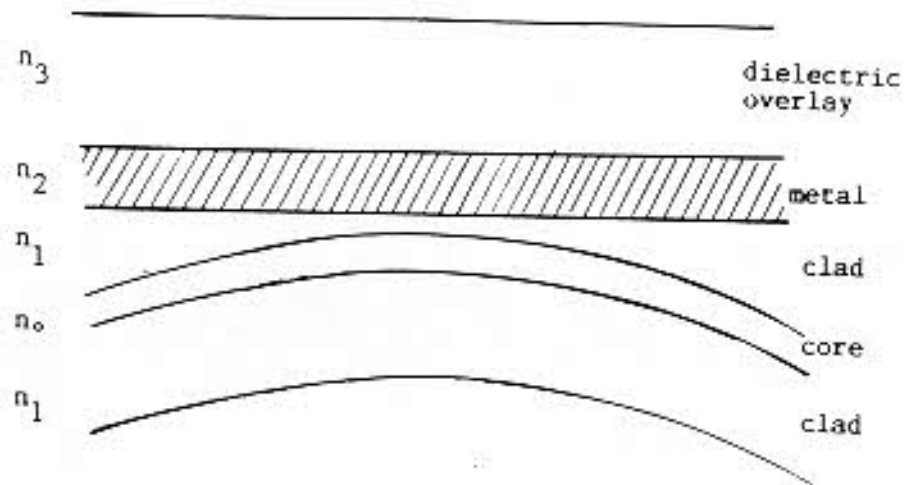


Fig.1-a Schematic diagram of polarizing structure

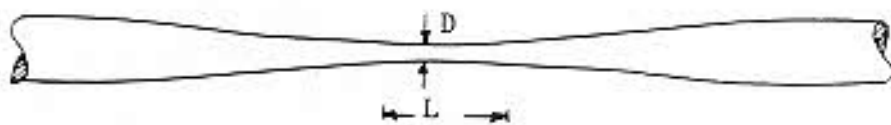


Fig.1-b Tapered fiber



Fig. 2 Experimental set-up

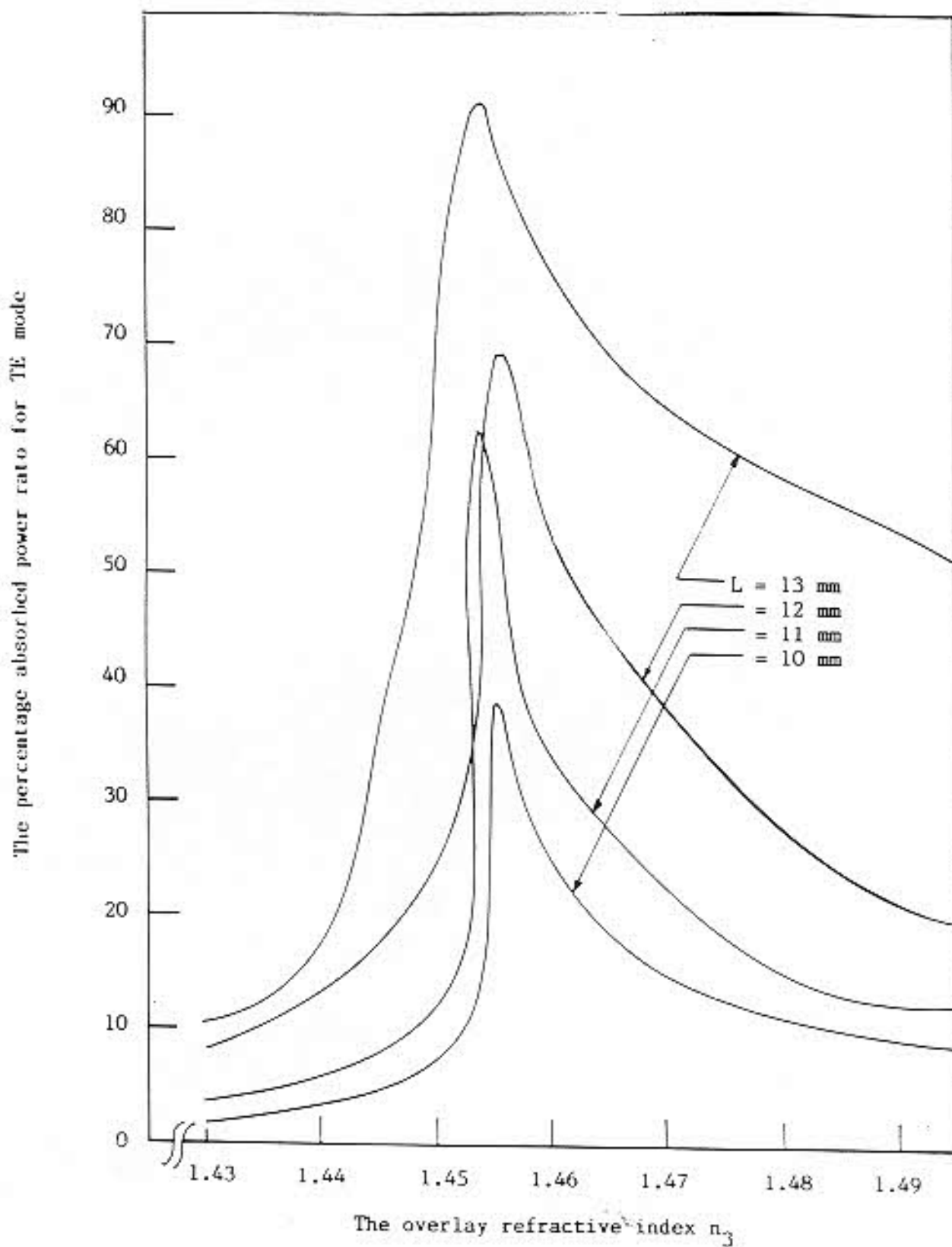


Fig.3 The absorbed power ratio with the overlay index for TE mode

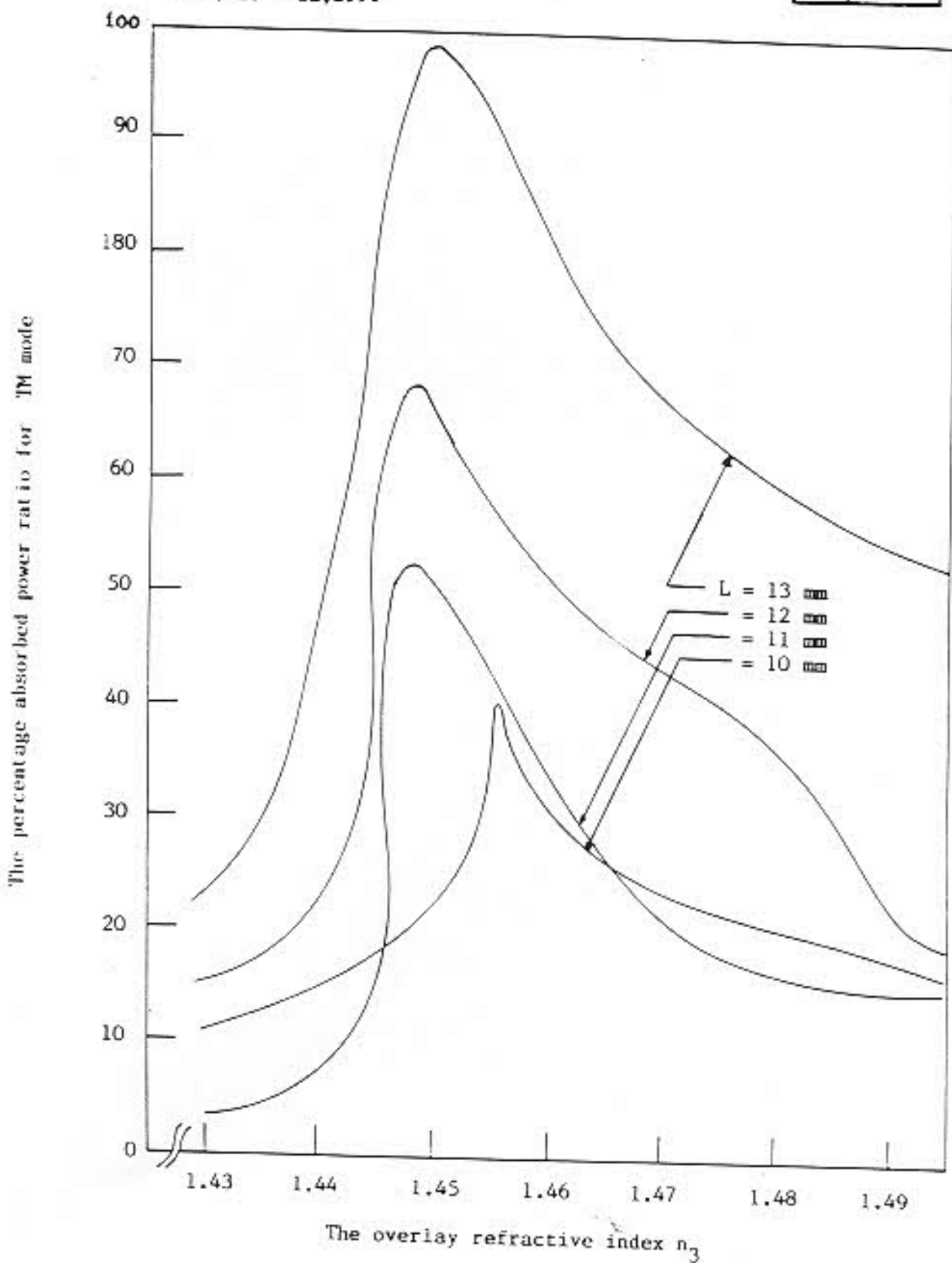


Fig.4 The absorbed power ratio with the overlay index for TM mode

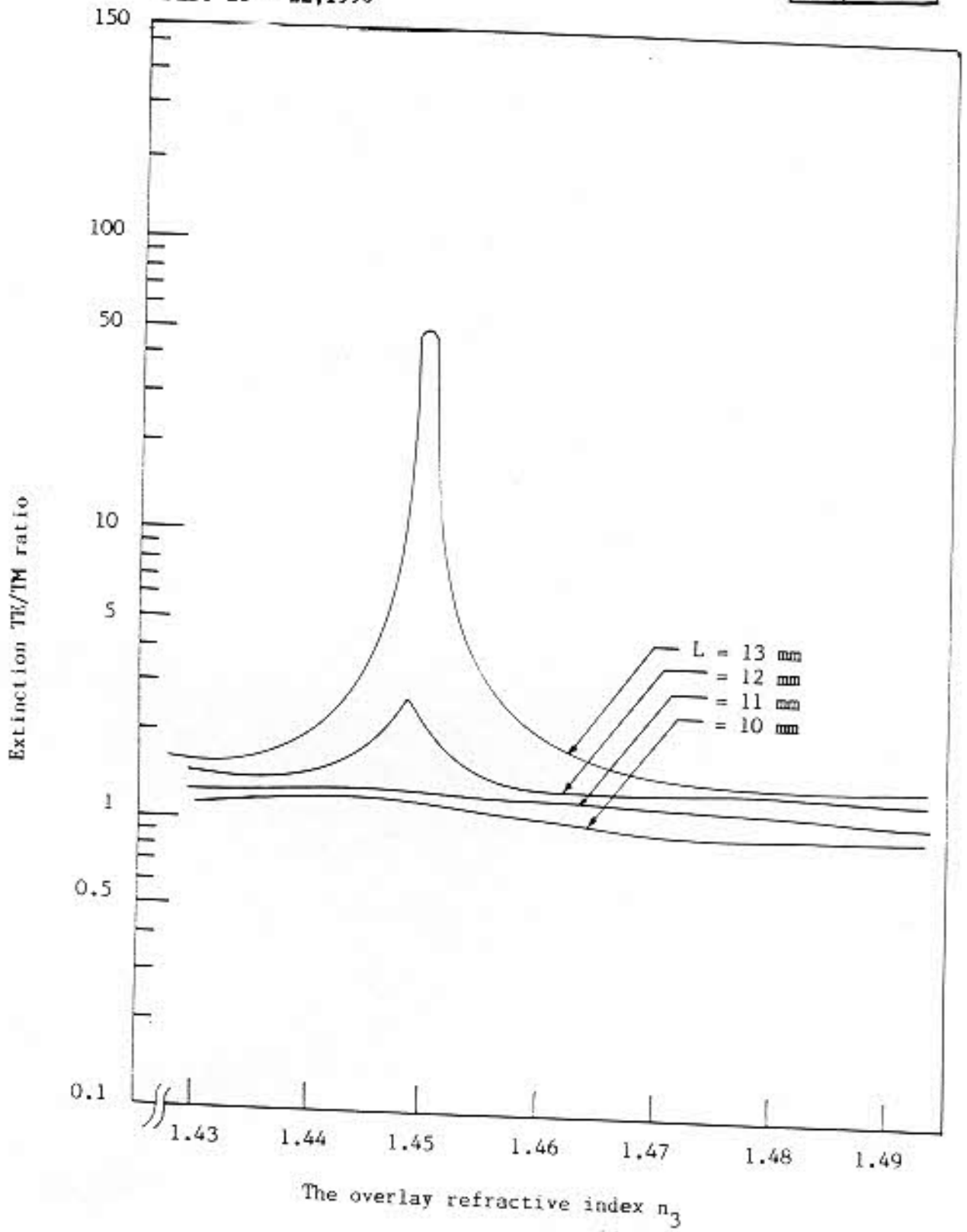


Fig.5 Observed TE/TM extinction ratio as function of overlay index